Submitted to American Chemical Society,
as a Monograph

LBL-5755
Preprint c.1

CROSSED MOLECULAR BEAM STUDIES OF FLUORINE CHEMISTRY

J. M. Farrar and Y. T. Lee

November 1976

Prepared for the U. S. Energy Research and
Development Administration under Contract W-7405-ENG-48

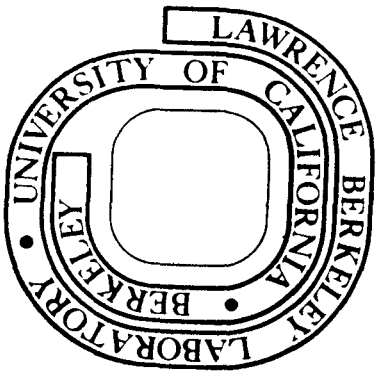

LBL-5755
c.1

DISCLAIMER

CROSSED MOLECULAR BEAM STUDIES OF FLOURINE CHEMISTRY

BY

J. M. Farrar and Y. T. Lee

Lawrence Berkeley Laboratory
University of California
Berkeley, California 94720

This work was done with support from the U.S. Energy Research and Development Administration.

CROSSED MOLECULAR BEAM STUDIES OF FLUORINE CHEMISTRY

J. M. Farrar and Y. T. Lee

Materials and Molecular Research Division
Lawrence Berkeley Laboratory

and

Department of Chemistry
University of California
Berkeley, California 94720

Introduction

Fluorine atom chemistry has received significant attention from chemical kineticists in recent years. Indeed, the present volume bears testimony to the proliferation of activity in this field. The molecular beam technique, which has come of age during the past several years, has been applied with great success to the chemistry of fluorine atoms and it is this subject which we will address in the present article. The crossed molecular beam technique (1) applied to problems in chemical kinetics involves colliding well-defined beams of atoms and molecules in a vacuum chamber; from the direct measurements of results of two-body collisions, in particular, angular and energy distributions of reaction products, one attempts to visualize in great detail how the reaction occurs. These dynamical features of chemical reactions, the favored orientation of molecules, reaction intermediate lifetimes, and product energy distributions are among the major concerns of a crossed molecular beam experiment.

The experimental results which we will describe are primarily those obtained in this laboratory but a few experimental data exist which have been collected elsewhere. Our experimental program in fluorine atom chemistry has been motivated primarily by two facts which have also been important to studies performed by other methods: (1) atomic fluorine abstraction of hydrogen atoms from appropriate molecules has been demonstrated to be an important class of reactions for chemical lasers (2). In particular, the reactions of $F + H_2 \rightarrow HF + H$ and $F + D_2 \rightarrow DF + D$ have been investigated in great detail by various theoretical and experimental approaches (3-11); the latter reaction provides us with an example from the general class of reactions of fluorine atoms with diatomic molecules. (2) Substitution reactions of fluorine atoms with unsaturated hydrocarbons involving the formation of C-F bonds frequently are observed to proceed through a "complex" which

lives many rotational periods (12-19). Since the C-F bond is the strongest single bond involving a carbon atom, these reactions are generally quite exoergic with cleavage of C-C, C-H, and C-Cl bonds occurring readily. Since many of these reactions do proceed through intermediates, the competition among various modes of bond cleavage in the long-lived intermediate yields valuable information on intramolecular energy transfer in the complex prior to decomposition to products. Various studies of reactions of fluorine atoms with hydrocarbons, both aliphatic and aromatic, as a function of substituent placement and identity, chain length, and initial kinetic energy of the reactants thus make the fluorine atom chemistry observed a very interesting probe of unimolecular decay. Many of the first studies of unimolecular decompositions from this laboratory were concerned with the determination of product branching ratios and recoil velocity distributions in olefins, aromatics, and heterocyclics at a fixed collision energy. Certain characteristic features of these reactions began to emerge in terms of the nature of the exit channel, that is, whether the critical configuration corresponded to a potential energy maximum or merely resulted from angular momentum, and the nature of the group emitted. Additional work on selected systems as a function of the initial collision energy has led to a further understanding of the role of the potential surface in unimolecular decompositions.

Experimental Method

The molecular beam technique, in general, is ideally suited to the study of reactions of highly reactive species such as fluorine atoms; since beam intensities and detector sensitivities are limited even under the most favorable experimental conditions, only for reactions with large cross sections and favorable kinematic relations can one hope to measure both energy and angular distributions of product molecules by crossing two well-defined reactant beams at a given collision energy. Since the internal states or the velocities of the reactants can be selected, the initial relative velocity vector can be well-defined in magnitude and direction and thus the measured quantities in a molecular beam experiment, the angular and energy distributions of scattered products, can be related to the mechanics of single collisions. The differential cross section for chemical reaction, which is the quantity most easily related to classical and quantum mechanical models based on collision theory and from a knowledge of potential energy hypersurfaces, is determined rather directly in a beam experiment, although present experimental data yield cross sections averaged to a great extent over initial impact parameter and final internal state distributions. This situation contrasts, however, with the much more highly averaged rate constant of classical kinetics which is an average over the initial Boltzmann distribution of the reaction cross section at a parti-

cular relative velocity weighted by the relative velocity. In principle the beam technique provides the means for studying state-to-state chemical kinetics on favorable systems, and highly refined experiments employing two crossed beams with specified internal states and relative velocities are definitely possible in the near future.

In molecular beam experiments, all measurements are carried out in a laboratory system of coordinates, but one wishes to interpret data in terms of a coordinate system which moves with the center of mass (c.m.) of the colliding system. The manner in which this transformation is made is well-understood (20-23), but the Jacobian involved in the transformation distorts certain portions of the lab data; in addition, the lab-c.m. transformation is often not single-valued. In order to circumvent this problem, data fitting routines have been developed which assume c.m. angular and velocity distributions, averaging them and transforming them back to the lab for comparison with the data. When the initial velocity distributions are quite narrow, this technique allows one to recover the c.m. distributions reliably. A velocity vector diagram shown in Figure 1 illustrates the nature of the transformation. The vector $\underset{\sim}{C}$, which points in the direction of the c.m. determined by partitioning the initial relative veocity vector according to conservation of linear momentum, allows us to relate laboratory velocity, $\underset{\sim}{v}$, and scattering angle, Θ, to c.m. velocity, $\underset{\sim}{u}$, and angle, θ, through the vector addition $\underset{\sim}{u} + \underset{\sim}{C} = \underset{\sim}{v}$. Since we determine $\underset{\sim}{v}$ and we desire $\underset{\sim}{u}$, we must deconvolute $\underset{\sim}{C}$. If the initial conditions create a substantial spread in vectors $\underset{\sim}{C}$, then the set of vectors $\underset{\sim}{u}$ which we determine to fit a measured $\underset{\sim}{v}$ are not unique. In fact, some experimental data have been interpreted incorrectly by failing to account correctly for the spread in initial conditions and also failing to use the correct Jacobian to relate lab and c.m. fluxes. We refer the reader to an earlier review (24) for further discussion of this point.

The development of a crossed molecular beam apparatus capable of the detection of arbitrary molecular fragments resulting from chemical reaction has been central to the advancement of molecular beam kinetics. The first reliable and sensitive apparatus of this sort employing electron-bombardment ionization of reaction products in an ultrahigh vacuum chamber followed by mass spectrometric detection became operational in 1968 (25) and a number of instruments of this type are now employed in various laboratories. This so-called "universal" detector together with the advent of free jet molecular beams (26) moved molecular beam chemical kinetics out of the "alkali age", so named because surface ionization detection techniques used previously limited the species to be studies to alkali atoms and alkali halides. The general experimental arrangement employed in a crossed molecular beam apparatus is shown in Figure 2. Reagent atomic species formed by thermal dissociation in a heated

oven are collimated into a beam; separate beam formation, collimation, and reaction chambers are used to insure that the beams are well-defined and, depending on the nature of their formation, do not present a large gas load to the collision chamber. The details of halogen-atom beam formation are discussed in greater detail below. The secondary beam of reactant molecules is formed in a similar manner and intersects the atomic halogen beam at 90° in a collision chamber maintained at 10^{-7} torr by an oil diffusion pump. Collisions then occur at the intersection zone of the beams; for measurements of angular distributions, reactively scattered products are detected in the plane defined by the beams as a function of laboratory scattering angle, Θ, by a rotatable mass spectrometer detector. This detector is comprised of three nested vacuum chambers, each pumped with a separate ion pump (and cryogenic pumping in the innermost chamber) to achieve a pressure of less than 10^{-10} torr in the ionization region. An electron bombardment ionizer of approximately 0.1% efficiency produces ions which are then injected into a quadrupole mass filter. While the pressure in the ionization region is ~10^{-10} torr, the partial pressure of reaction products may be as low as 10^{-15} to 10^{-16} torr when they reach ionization region. At such low signal levels, very careful work must be done to extract meaningful signals, including mechanical design to eliminate sources of background molecules in the detector, elaborate cryogenic pumping, and beam modulation techniques as discussed below. After the ions pass through the mass filter, they are accelerated and collimated into a beam which is directed to an aluminum coated cathode held at -30 kV. Several secondary electrons are emitted per incident ion; these electrons are accelerated in the same 30 kV potential to a Al coated plastic scintillator which emits several photons per secondary electron. The photon pulses are amplified by a photomultiplier tube and counted using conventional techniques. As indicated above, beam modulation is used for low-level signal recovery and to effect this, the secondary (molecular) beam is chopped with a tuning fork at 150 Hz. A signal from the chopper is processed by a digital logic circuit which gates a dual scaler in synchronization with the beam modulation. In this configuration, one scaler counts signal plus background corresponding to the beam open period; the other scaler collects background only. In this manner, reactive scattering signals which generally range from a few counts per second to several hundred per second can be recovered.

The total energy of the system under study consists of the initial relative and internal energies plus the exoergicity of the reaction. This energy can be divided among internal degrees of freedom plus relative translational energy of the products. In our molecular beam experiments, we measure velocity distributions of scattered products to infer internal energy distributions by conservation of energy. On the other hand, detailed

state distributions for some simple diatomic product molecules could be measured by using the molecular beam resonance method (27,28) or laser-induced fluorescence (29,30).

Velocity distributions of the reactively scattered products can be measured by time of flight (TOF) methods in which the velocity of a particle is determined by measuring the time required for the particle to traverse a known distance in the detector. Although not indicated in Figure 2, a chopper with very narrow slits chops the reactively scattered products as they enter the detector at a frequency (1600 Hz, typically) which is high compared to the secondary beam modulation frequency. The burst of molecules then enters the detector at time t_o and the pulse spreads in time during transit through the detector in accordance with the velocity distribution of molecules in the pulse. A multi-channel scaler then records the distribution of flight times of the products; signal averaging is accomplished by minicomputer control of the TOF unit. Flight times of 100-400 μsec through our detector (pathlength 17 cm) are measured quite readily using this technique.

Having discussed in general terms how angular and velocity distributions of reactively scattered products are measured using a "universal" molecular beam apparatus, we now focus attention on methods of beam production, in particular, techniques for the production of stable, intense beams of fluorine atoms. Since the bond energy of F_2 is 36 kcal $mole^{-1}$, thermal dissociation of F_2 in a heated nickel oven has been found to be a successful method for fluorine atom production. The high reactivity of fluorine atoms with various materials rules out a great number of them for oven construction and we have found that nickel affords the best readily available material. Thermal dissociation of F_2 in a nickel oven at a pressure of ~0.1 - 1.0 torr at 750°C can be accomplished with the degree of dissociation approaching 50 - 90%. At such low pressures, beam formation is determined by effusion through an orifice and the velocity distribution of the atoms is the Maxwell-Boltzmann distribution. In the absence of velocity selection, such a broad distribution of initial speeds leads to a very broad distribution of initial kinetic energies, with the relative velocity vector and the center of mass vector distributed over a large region of velocity space. A slotted disc velocity selector (31) can be used to reduce this spread in initial conditions and much of the work discussed in this paper was performed with such a selector with a full width half maximum (FWHM) velocity spread of 20%. Such a small spread in the initial relative velocity of the reactants enables the lab - c.m. transformation to be made more uniquely, thus assisting us in the interpretation of the data.

The velocity selected fluorine atom source was the workhorse for much of the work done in this laboratory, but recent developments in seeded supersonic beam technology have led to much more efficient means of halogen atom beam production. The

expansion of a gas at a few hundred torr through a small orifice into a vacuum has been shown to be an effective means for the production of high intensity, narrow velocity spread atomic and molecular beams. By mixing 1 to 2% F_2 with a rare gas carrier such as argon or helium and expanding the mixture at 500 torr through an orifice (0.1 mm dia) in a nickel oven heated to 750-800°C, fluorine atom beams were produced which were one to two orders of magnitude more intense than velocity selected beams and had velocity distributions which were somewhat narrower than selected beams, generally with a 15% FWHM spread. Such a method of beam production maintains the low partial pressure of halogen to make the equilibrium favor atom production while providing a high pressure expansion under hydrodynamic flow conditions leading to a narrowing of the velocity distribution.

Under the hydrodynamic flow conditions of supersonic expansions, species of different masses in a molecular beam achieve the same terminal velocity which is related to the average mass number of the expanding species. This technique can be used to increase the speed of a heavy particle relative to its thermal speed if a small fraction of the gas mixture is the desired heavy species and the bulk of the mixture is a light carrier gas. This technique has been used very successfully to produce hyperthermal beams of Xe atoms formed by expansions of mixtures composed of 1% Xe in 99% H_2. By varying the diluent gas from argon to helium, high energy beams of fluorine atoms can be produced for reactions in the hyperthermal region (10-40 kcal $mole^{-1}$).

This technique of halogen atom production is not unique to fluorine; in fact, the first halogen atom beam produced in this laboratory was a chlorine atom beam produced by dissociation of Cl_2, in argon buffer gas in a heated graphite oven (32). The technique should be applicable to all of the halogen atoms and a vast variety of scattering experiments can be initiated using such sources.

The molecular beams in our experiments are also formed by supersonic expansion. In addition to enhanced intensity and narrow velocity distributions obtained in this way, the molecules in such beams can generally be considered to be in their lowest vibrational and rotational states. This "freezing out" of internal degrees of freedom is important in further defining the initial experimental conditions. In understanding the mechanics of collisions, one can obtain simplifications in interpretation by knowing that reactant molecules are rotationally and vibrationally "cold". This point will be discussed further in later sections of this paper.

Examples of Experimental Results

I. $F + D_2 \rightarrow DF + D$. The reaction of atomic fluorine with molecular hydrogen containing molecules has been demonstrated to

be the chief mechanism responsible for the HF chemical laser and has received significant experimental and theoretical attention. In addition to chemical laser (2,11,33,34) and infrared chemiluminescence (5,6) measurements on this system which have yielded values for a number of rate constant ratios for production of specific vibrational states of HF, the molecular beam technique (3,4) has also provided significant data on this reaction. The $F + D_2$ reaction to form DF is exoergic by 31.5 kcal $mole^{-1}$, yielding enough energy in conjunction with translation to produce DF in excited vibrational states up to $v' = 4$. The equal gain and zero gain variations of the chemical laser technique (2) allow for the determination of rate constant ratios $k_{v'}/k_{v'-1}$ for $v' = 1, 2, 3$, and 4 where v' is the DF vibrational quantum number and infrared chemiluminescence measurements allow for determinations of this ratio for $v' = 2$-4. In contrast, the crossed molecular beam technique is not very ideal for measurements of relative state populations although, as we shall see, some information of this type can be determined under favorable conditions.

The laws of conservation of energy and angular momentum play a very important role in determining what information is contained in the molecular beam data on this system. A consideration of rate constant data (35) for this system in conjunction with the recognition that the rate constant is an ensemble average of cross section weighted by relative velocity, allows us to estimate the maximum impact parameter contributing to chemical reaction. At 300°K, the cross section is $\lesssim 1$ Å^2 so b_{max} is roughly 1 Å. For an impact parameter of 1 Å and v_{rel} $\sim 2 \times 10^5$ cm sec^{-1} (for a collision energy of 1.7 kcal $mole^{-1}$), $L = \mu v b$ or approximately $10\hbar$ in magnitude. Since at room temperature, J, the rotational angular momentum of D_2, is no more than $2\hbar$, we can use the conservation relation, $\underset{\sim}{J} = \underset{\sim}{L} + \underset{\sim}{j} = \underset{\sim}{L}' + \underset{\sim}{j}'$, to allow us to conclude that J' is likely to be small also (10-$12\hbar$). Since the exit channel reduced mass is small, even if all of the initial orbital angular momentum appears as product rotational excitation, the rotational energy of DF will be approximately 3 - 5 kcal which is less than the vibrational level spacing of 8 kcal. Thus, by conservation of energy, only discrete regions of product translational energy space will be populated and "quantization" of the product velocity distribution should occur. In a crossed beam experiment with well-defined beam velocities, one thus expects significant structure in the product velocity spectrum. Under very favorable kinematic circumstances, particularly at low collision energies where the angle between $\underset{\sim}{V}_{rel}$ and $\underset{\sim}{V}_{D_2}$ is quite large, such structure should also be observable in the angular distributions. Figure 3 demonstrates this point clearly. Two discrete peaks are observable at both the collision energies; the lower panel of this figure shows Cartesian plots corresponding to these experiments. The significant feature of both of these contour maps is that the DF

product scatters predominantly in the backward direction in the c.m. system, corresponding to net repulsive encounters; as the collision energy is increased, the sharpness of the backward scattering diminishes and products are formed scattered through angles significantly smaller than 180°.

Experiments performed at higher collision energies continue to show the trend toward more forward scattering, but the predominance of backward scattering is still in evidence. While all of the experimental data show structure arising from individual vibrational states of DF, determination of rate constant ratios is very difficult since one must integrate flux over c.m. velocity to assess these ratios. The $1/u^2$ Jacobian singularity near the c.m. is most pronounced in calculating the k_4/k_3 ratio and the centroid distribution, although narrow by contemporary standards, is broad enough to introduce prohibitively large uncertainties into calculations of relative populations.

The observation of DF predominatly scattered into the backward hemisphere at the collision energies studied here suggests that the favored orientation for reaction is collinear. Ab initio calculations of the potential energy surface for this system (10,36) suggest that collinear approach of $F + H_2$ is the dominating geometry leading to chemical reaction. Indeed, the backward scattered DF product is that which one expects from low impact parameter collisions. One can thus conclude that the beam data are consistent with a potential energy surface with predominant collinear character. For simple systems containing light atoms, the comparison between theoretical studies and experimental results will provide further understanding of reaction dynamics from first principle in the very near future.

II. Substitution Reactions of F Atoms with Unsaturated Hydrocarbons.

A. General Remarks on Unimolecular Decompositions of Chemically Activated Radicals. A major portion of the molecular beam studies of fluorine atom chemistry (12-19,37) has been concerned with a class of reactions characterized by the formation of a transient species from bimolecular association of the reactants and whose lifetime is long compared to its rotational or vibrational periods. The formation of such a long lived complex implies that the reactants experience a net attraction and consequently the potential energy surface for the reaction possesses a deep well; of course, the total energy of the system is greater than that required to dissociate the intermediate, either to reactants or products, so that in the absence of a third body or relatively improbable photon emission (radiative lifetime $\gtrsim 10^{-2}$ sec), the intermediate must decay prior to detection. Under certain favorable conditions where a large

number of internal degrees of freedom participate in the redistribution of the excitation energy, the reactive intermediate could live long enough to travel to our detector, but none of the systems studied to date have exhibited this behavior.

The decay of a complex formed in such a bimolecular encounter provides us with an example of the general class of reactions denoted as unimolecular decompositions (38). Under circumstances in which a long-lived complex decomposes to products, a vast collection of questions can be asked regarding the dynamics of the decomposition, including the extent to which the initial excitation energy of the intermediate species is distributed throughout the entire molecule before a sufficient amount localizes in the bond to be broken as the products form. The most widely accepted model of unimolecular decay, the Rice-Ramsperger-Kassel-Marcus (RRKM) theory (38,39), states that a quasiequilibrium between the complex and the initial configuration is maintained through the reaction. This assumption is equivalent to stating that energy randomization in the complex is rapid compared to chemical reaction. The technique of chemical activation developed by Kistiakowsky (40) and extensively employed by Rabinovitch and co-workers (41) has provided kineticists with a large body of experimental data, the majority of which lend support to the assumptions of RRKM theory. In this technique, the complex is "synthesized" in a bulb reactor by a bimolecular reaction and the ratio of the concentration of complexes stabilized by collisions with background gas molecules to products of decomposition is measured as a function of pressure. Under these circumstances, the "clock" for these experiments becomes the time between collisions and if one assumes that the "strong collision" assumption is valid, that is that an activated molecule (one with enough energy to decompose) can be deactivated in a single collision with a buffer gas molecule, one can infer whether or not the product yields are characteristic of a statistical distribution of energy in the complex. Direct comparisons with RRKM theory can be made since this model is concerned with complex lifetimes and rates of decomposition, quantities which these conventional kinetic methods determine directly.

Information of a different sort is obtained in a molecular beam experiment, although the means for producing the species undergoing unimolecular decomposition is also chemical activation. Whereas the conventional kinetic studies yield reaction rates for direct comparison with RRKM lifetimes, the beam technique yields product recoil energy distribution which, in principle, contain information regarding exit channel dynamics specifically ignored in RRKM. Comparison of experimental results with RRKM theory is indirect, requiring additional assumptions whose validity must be determined. Fortunately, however, statistical theories of a different sort exist which base their predictions on asymptotic (and therefore measureable) properties of the

products; these "phase space" theories (42,43) will be discussed in greater detail below.

Reactions studied using the chemical activation technique in beam or bulb experiments yield important information because the intermediate radicals have well-defined excitation energies; unimolecular decompositions involving the formation of a C-F bond have additional appeal because many competing channels for decomposition open up and studies of branching ratios for C-H, C-C, or C-Cl bond cleavage provide important chemical information. In a statistical model, the rate for a particular channel is proportional to the density of states at the critical configuration; consequently, one expects that more exoergic reactions should proceed with greater rates since more states are accessible under such circumstances.

In the discussion of specific experimental systems which follows, the bulk of our remarks will be limited to a discussion of product recoil velocity distributions and the information which such studies provide for us. An understanding of the energetics of unimolecular decomposition and their relation to product velocity distributions can be facilitated by referring to Figure 4. The excitation energy of the complex, E^*, is determined by the initial translational and internal energy of the reactants plus the well depth of the complex. Unimolecular decomposition to products can occur when energy E_o flows into the reaction coordinate such that the barrier V_a is surmounted. This barrier can include centrifugal energy plus potential energy terms; whenever terms of the latter type are present, the critical configuration is "tight", that is, incipient product rotations are not free, but correspond to bending vibrations (44). This potential energy barrier implies that the reverse association reaction has a nonzero activation energy; the nature of this barrier and its disposal as product translation and internal energy is a vital factor in interpreting measured product recoil distributions. The energy in excess of the critical configuration barrier, $E_T - V_a$, where $E_T = E_{trans} + E_{int} - \Delta D_o^o$ is the total available energy, is that quantity of energy which can be distributed among the various product oscillators plus the relative translational energy of the separating fragments. If some energy $\varepsilon^\dagger$ at the critical configuration is apportioned to the coordinate which becomes product translation, then $\varepsilon^\dagger$ should be a lower bound to the translational energy of the products. The manner in which the exit channel barrier releases its energy V_a among product degrees of freedom is a dynamical consideration not addressed by conventional RRKM theory, although recent efforts to include these dynamics in a "tight" transition state theory have been made (45). In the case where the critical configuration is tight, the product recoil distributions cannot be predicted by RRKM theory and any assumptions which one makes to connect the energy distribution at the critical configuration with that of reaction products must be assessed carefully. Certain

trajectory calculations (46) formulated to probe energy release from such a repulsive force in the exit channel suggest that when a light atom is emitted from a complex, such as during C-H bond cleavage, most of the exit channel barrier V_a appears in product translational energy. While such an energy transfer mechanism is valuable in interpreting our experimental data, we feel that one should avoid using RRKM theory without considering the exit barrier to predict product recoil energy distributions.

Other models have been formulated which predict product recoil energy distributions, most notably the phase space theory of Light and co-workers (42,43). This model possesses the desirable attribute that cross sections are computed by evaluating the volume in phase space which the products can sample which is accessible from a statistical complex whose conserved quantum numbers are given by the total energy, the total angular momentum and its projection on a space-fixed axis. Thus the theory is parameterized in terms of the observable properties of product molecules; however, establishment of the limits on the formation and decomposition of a strong-coupling complex frequently necessitates considerations of intermediate geometry, particularly when the rotational energy of the complex must become product angular momentum under the dictates of an exit channel barrier. A number of variations on the phase space theory have been proposed and the literature can be consulted for details (16).

A comparison of RRKM and phase space theory indicates that the degree and philosophy for parameterizing these models is quite different. In the former case, the only constant of the motion is the total energy of the system. Phase space theory is appealing because two more constants of the motion corresponding to angular momentum variables have been considered in the derivation. The recent versions of transition state theory which consider explicitly angular momentum in limiting cases where the total angular momentum becomes either product rotational or orbital angular momentum yield results in accord with phase space theory (45). The various models for product recoil distributions can be illustrated most fruitfully by consideration of several systems to which we now turn.

B. $F + C_2H_4$. A system which has received substantial attention in molecular beam experiments in this laboratory and which provides us with an opportunity to discuss many of the important features of unimolecular decay is the F + C2H4 reaction (12,19). The reaction to form C_2H_3F plus a hydrogen atom is exoergic by approximately 14 kcal $mole^{-1}$ and the stability of the intermediate radical, C_2H_4F, is estimated to be ~50 kcal $mole^{-1}$ with respect to reactants. A molecular beam experiment performed as indicated in the previous section, then, reveals the characteristic formation of the C_2H_3F product near the direction of the center of mass of the system, as shown in Figure 5. Velocity analysis of the reaction products confirms

the symmetry of the product emission about $\theta_{c.m.} = \pi/2$ as expected for a complex which lives many rotational periods. Initial angular and velocity distribution measurements on this system yielded valuable information on the c.m. angular and energy distributions with the following notable points: the c.m. angular distribution measured at the relative collision energy of 1.98 kcal mole^{-1} was symmetric about $\pi/2$ as expected, but the distribution was peaked at $\pi/2$ in the c.m. system. This peaking was explained by considering the angular momentum disposal in the chemical reaction: while the explanation has appeared in detail in previous publications (18), we repeat the salient features here. Recalling that the total angular momentum must be conserved in a collision, we note that since the C_2H_4 molecules are produced in a nozzle expansion and are therefore rotationally "cold", the initial orbital angular momentum then becomes the total angular momentum of the system and will be perpendicular to the initial relative velocity vector. During the lifetime of the complex, the total angular momentum is the rotational angular momentum of the complex, which rotates in the plane defined by the heavy atom C-C-F framework. As the C-H bond extends and breaks along the reformed p_z orbital on the sp^2 hybridized carbon atom, the emitted hydrogen atom is emitted along the rotational angular momentum vector. This vector becomes the final product rotational angular momentum since the emitted hydrogen atom cannot remove a significant amount of orbital angular momentum. We thus see that the products recoil along $\underset{\sim}{J}'$ which is perpendicular to $\underset{\sim}{V}$, thus producing the observed sideways peaking. A second notable feature of the observed c.m. distributions is found in the c.m. energy distribution: the shape of the distribution is quite wide and yields an average product kinetic energy which is ~50% of the total available energy, far in excess of statistical predictions. The interpretation of this result at a single collision energy is complicated by the fact that hydrogen addition to a halogenated olefin on the end of the molecule where the halogen resides proceeds with an activation of energy of ~3 kcal mole^{-1} (47), therefore suggesting that the exit channel for the C_2H_4F decomposition to C_2H_3F + H has a barrier. The manner in which energy is released in descending this barrier then destroys the energy distribution at the critical configuration which RRKM theory predicts. A contour map of c.m. product flux as a function of polar coordinates (u,θ) is shown in Figure 6.

In order to provide further insight into the perturbation of the critical configuration energy distribution by the exit barrier, additional experiments on this system at higher collision energies have been undertaken. The seeded beam technique can be used to vary the collision energy from 2.2 kcal mole^{-1} to 12.1 kcal mole^{-1}, thereby increasing the total energy available to the system from 16 to 28 kcal mole^{-1}.

The determination of the initial collision energy dependence of the unimolecular reaction dynamics can in principle, provide

two kinds of information. Since the energy which can be distributed amoung the various modes of the critical configuration is the total available energy in excess of the barrier, increasing this total energy should minimize the nonrandom contribution of V_a to P(E') as E_T increases. Thus, if a statistical model is correct and requires corrections arising from the specific dynamics associated with V_a, then as the collision energy is increased, P(E') should approach statistical behavior more closely. This is the information which we seek in the C_2H_4F system. In principle, information of a different sort can be obtained from the initial collision energy dependence of $g(\theta)$, the c.m. angular distribution function. When the binding energy E_o of the chemically activated intermediate becomes comparable to the collision energy, the complex lifetime should approach one rotational period and the $g(\theta)$ function should lose its symmetry about $\pi/2$. By then estimating the rotational period of the complex, one can then infer the complex lifetime. If one then knows accurately the stability, E_o, of the complex, model calculations to test statistical theories of unimolecular decay can be made. This experimental handle on the decay of a long-lived complex yields lifetimes which can be compared directly with quantities to which RRKM theory addresses itself directly. This desirable state of affairs is generally not achieved in beam experiments on chemically activated radicals; the large stability of the intermediate complex (~30-60 kcal $mole^{-1}$) compared to available collision energies in our experiments does not allow us to use the rotational period as a "clock". The C_2H_4F system, however, does allow us to use the first method for separating the role of the exit channel barrier in the measured recoil energy distributions.

The experimental data obtained over the range of collision energies 2.2 to 12.1 kcal $mole^{-1}$ are shown in Figure 7. Over this range of collision energies, the reaction appears to proceed through a long-lived complex, as evidenced by angular distributions symmetric about $\pi/2$ in the center of mass coordinate system. The sideways peaking noted in the earlier work is observed at all energies here, suggesting that the fractional partititioning of the total angular momentum into rotational and orbital angular momentum remains constant. The significant conclusion from these experimental data, however, is that the recoil energy distributions maintain a rather constant shape as a function of the initial kinetic energy, channeling ~50% of the total energy into translation of the products. A comparison of the measured average kinetic energy of the products with calculations performed with various statistical models is quite instructive. We have performed phase space calculations of the recoil energy distributions including the phase space volume associated with all of the product vibrational modes and with a selected subset of product vibrational modes; the former calculation, denoted "12-oscillator"

model yields average kinetic energy releases which place a smaller fraction of the total energy into translation as the total energy increases. The latter phase space calculation in which the phase space volume associated with 5 product oscillators including only those modes expected to be active based on gross geometry changes during the reaction yields results in closer accord with experiment, but still somewhat discordant. This model, which heuristically incorporates partial activation of product oscillators, places a larger fraction of the total excess energy in translation since fewer oscillators share the energy, but again, the fraction of the total energy appearing in translation decreases at higher energies, in contrast to the 50% value observed at all energies. A third model, recently proposed by Marcus (45) accounts for the nature of the "tight" critical configuration by assuming that the quantum numbers for the bending vibrations in the transition state which become product rotations are "adiabatic on the average". This model then channels additional energy into translation since the energy of a bending vibrational quantum is greater than for a rotational quantum, the deficit accounted for by translation; calculations with this model yield results quite similar to the 12-oscillator phase space calculation. The statistical models, then, yield values of the average kinetic energy which are neither qualitatively or quantitatively correct. In all cases, the models place too little translational energy in the products and the fraction of the total energy appearing in translation decreases with increasing collision energy. The 5-oscillator phase space model yields results in closer accord with experiment, but this model certainly cannot be correct because a calculation of the complex lifetime performed using the density of states of these vibrations yields lifetimes which are smaller than one rotational period at all collision energies. Since the experimentally observed angular distributions place a lower bound on the lifetime of the complex of several rotational periods, we can be sure that the C_2H_3F recoil energy distributions cannot be explained by simple reduction of the number of oscillators participating in the decomposition.

Rowland (48) has studied the C_2H_4F system by measuring the pressure dependence of the stabilization-decomposition ratio for C_2H_4F produced in the hot atom reaction of $^{18}F + C_2H_4$; his results suggest that the lifetime of the complex is on the order of 10^{-9} sec, a result which can only be explained easily by including all of the complex's vibrations in a lifetime calculation. An explanation of the lifetime results and the recoil distributions must certainly require an explicit treatment of the dynamics of intramolecular energy transfer connecting the complex with the critical configuration. The normal modes associated with formation of the C_2H_4F complex are quite different from those required to form the products

(49); slow energy migration between those two subsets of oscillators might explain the long observed lifetime while the participation of a reduced set of vibrational modes in the decomposition may account for the disproportionately large fraction of the total energy in product translation. While the mechanical explanation for the large average kinetic energy release in this system has not yet been developed, the study of this reaction as a function of initial collision energy suggests strongly that the exit channel barrier does not account for the nonstatistical distribution of the excess energy.

C. The Effect of Potential Energy Barrier in the Exit Channel. We have indicated in the previous section that exit channel interactions can play a significant role in determining the translational energy distribution of product molecules. In the decomposition of C_2H_4F, we have demonstrated that to a large extent, the effect of the barrier can be minimized by studying the energy dependence of the product recoil distribution. A number of important points can be made regarding the systematics of the exit channel barrier by considering the decompositions of substituted fluorobenzenes. Table I and Figure 8 show the energetics associated with a number of these reactions and Figure 9 portrays some of the recoil distribution results graphically.

Table I

Energetics and Average Product Translational Energies, Fluorine + Substituted Benzenes

Reactants	Products	Exoergicity kcal mole^{-1}	Barrier kcal mole^{-1}	<E'> kcal mole^{-1}
$F + C_6H_6$	$C_6H_5F + H$	13	~4	7.7
F + toluene	$C_7H_7F + H$	13	~4	6.8
	$C_6H_5F + CH_3$	22	~7.5	9.3
F + m-xylene	$C_8H_9F + H$	13	~4	7.8
	$C_7H_7F + CH_3$	22	~7.5	11.0
$F + C_6H_5Cl$	$C_6H_4ClF + H$	13	~4	8.2
	$C_6H_5F + Cl$	29	~1	3.4

A number of conclusions can be reached from an examination of these data. We find that average product translational energy does not correlate well with reaction exoergicity. In

the case of Cl emission, this very exoergic channel results in only 3.4 kcal $mole^{-1}$ in translation whereas the less exoergic H-atom emission reactions result in much higher translational energy release. Higher still are the translational energy releases associated with CH_3 emission which are accompanied by very large exit channel barrier. One is immediately led to the conclusion that the energy released in descending the barrier is channeled primarily into product translation; very high translational energy release is found in CH_3 emission where a large barrier is expected, whereas Cl emission proceeds with very low translational excitation in accordance with a very small exit channel barrier. Hydrogen atom emission provides an intermediate case in which a 4 kcal barrier releases energy into translation with <E'> lying between values found for CH_3 or Cl emission.

One can therefore conclude that predictions of product energy distributions from the decompositon of long-lived complexes must first consider the height of the exit channel barrier. Most reactions under consideration here have exoergicities of 20 kcal or less; if the total excess energy of the complex is distributed randomly, then only ~1-2 kcal can be expected in the reaction coordinate if more than 10 vibrational degrees of freedom share the energy. Consequently, a barrier of height 5 to 10 kcal could channel much more energy than the statistical amount into product translation. For different reactions with comparable exoergicities, one thus expects that the higher the exit channel barrier, the "colder" the products.

Angular momentum conservation plays an important role in many of these unimolecular decompositions, particularly at higher collision energies. In the case of decompositions involving emission of a hydrogen atom from the collision complex, the light atom cannot remove significant orbital angular momentum and consequently initial orbital angular momentum become product rotational excitation. Consequently angular momentum conservation does not place kinetic energy restrictions on the product energy partitioning and one expects this kinematic freedom to hold at higher collision energies. In the case of heavy particle emission, however, the conservation laws can play a very important role. Earlier in this section we have discussed the conversion of exit channel potential energy into translation; one should also note, however, that when this energy is released along a line which does not pass through the center of mass of the collision complex, substantial product rotational excitation can occur, particularly if the moments of inertia are large. Under these circumstances product orbital angular momentum might be substantially decreased thereby removing restrictions on the recoil energy distribution. Conversely, if significant orbital angular momentum is carried away by the products, reduced masses

and interaction potential ranges might require that a large fraction of the rotational energy of the complex be carried away as product translation such that recoil velocities might be larger than one initially expects from simple statistical factors. In particular, the "hot atom preparative conditions" discussed by Bunker (50) regarding unimolecular decomposition of species formed from translationally "hot" reactants may play a very important role in decomposition lifetimes and recoil energy distributions. If an activated molecule is formed from high angular momentum reactants, its decomposition may be significantly governed by conservation laws; especially when the total angular momentum is placed into final orbital angular momentum, we expect translationally "hot" products to be formed. This situation should be particularly marked in cases where a slight activation energy for the reaction causes the total cross section to increase with collision energy. Under such circumstances, the initial orbital angular momentum increases dramatically with energy and its conversion into product orbital angular momentum requires the mean velocity with which the products retreat from one another to increase dramatically. The net effect of the conservation laws then is to force the average fraction of the total energy in translation to increase with collision energy, in opposition to the usual statistical result. This point is shown more clearly in the F + CH_3I reaction discussed in the section immediately following.

III. Other Examples

A. F + $CH_3I \rightarrow IF + CH_3$. This chemical reaction provides us with an example of an abstraction reaction from an aliphatic compound; three channels are open in this system as indicated here:

$$F + CH_3I \rightarrow IF + CH_3 \qquad \Delta H = -11 \text{ kcal}$$

$$\rightarrow HF + CH_2I \qquad \Delta H = -35 \text{ kcal}$$

$$\rightarrow CH_3F + I \qquad \Delta H = -53 \text{ kcal}$$

The last reaction, while highly exoergic, has been found by Tal'rose (51) to be of negligible importance in this system; the second reaction is known to produce vibrationally excited HF yielding laser action, but we have not studied this channel. Tal'rose has also studied the reaction to produce IF using mass spectrometric probing of fluorine flames and has measured a rate constant $k = 2 \times 10^{-10}$ cm^3 sec^{-1}.

We have studied the IF production reaction (37) at two collision energies, 2.6 and 14.1 kcal $mole^{-1}$ produced by Ar and He seeded F atom beams; the laboratory angular distribution for

IF at the lower collision energy in Figure 10 shows some symmetry about the centroid, suggesting that the reaction proceeds through a long-lived complex. The time of flight data in conjunction with the laboratory angular distribution data indeed confirm that the c.m. angular distribution is symmetric about $\theta = \pi/2$ as expected from decomposition of a complex which lives many rotational periods. The angular distribution in the center of mass system is of the form $(1 + a \cos^2\theta)$, symmetric about $\pi/2$ but anisotropic, thereby providing information about angular momentum partitioning in the decomposition of the complex. In particular, the strong forward-backward peaking at this collision energy indicates that the complex is quite prolate, which is not surprising since CH_3I is a highly prolate (cigar-shaped) symmetric top, and that the complex rotational angular momentum becomes product orbital angular momentum. This situation occurs, as pointed out by Miller, Safron, and Herschbach (52), because the creation of products with low rotational excitation in conjunction with the azimuthal symmetry of $\underset{\sim}{L}'$ about $\underset{\sim}{V}'$ causes the product $\underset{\sim}{V}'$ vectors to map out a sphere and the intensity of products "piles up" at the poles. This situation is relatively common in alkali atom-alkali halide exchange reactions in which long range forces created by dipole-polarizable atom interactions make L and L' large; the F + CH_3I case, however, is unique in that the forces are relatively short range. The disposal of angular momentum in this case is governed by the highly prolate nature of CH_3IF.

The recoil distribution for this system is rather interesting; we find that the products are formed with ~30% of the total energy in translation. This result is quite close to statistical predictions and, in fact, the phase space volume associated with the high frequency H-atom motions in the CH_3 fragment is so small that the experimental data do not allow one to conclude the extent to which vibrational energy is shared among the modes of the collision complex.

At higher collision energy the angular distribution in Figure 11 shows quite dramatically the forward-backward peaking mentioned previously. Now, however, the peaks are not of equal intensity in the c.m. system; this result would be expected if the collision complex lived only a fraction of a rotational period. One can convolute the random lifetime distribution expected for the decomposition with the classical angular momentum form factors to relate the ratio of the forward-backward intensities to the rotational period of the complex. This "osculating" model (53) predicts that a forward-backward ratio of ~1.5 corresponds to a complex lifetime of half a rotational period. Based on estimates of the total reaction cross section, we can compute the maximum orbital angular momentum quantum number leading to reaction and compute a rotational period of 8×10^{-12} sec. A comparison of this lifetime with RRKM theory

indicates that the "observed" value lies between predictions based upon full activation of the CH_3 vibrations and activation of the ν_2 mode only. However, this variation is less than an order of magnitude and one must thus conclude that this system does not allow us to make a sufficiently sensitive test of the energy randomization hypothesis in RRKM theory.

Phase space calculations of the product recoil energy distributions are shown in Figure 12 and yield much the same conclusion regarding the role of high frequency vibrations in determining these quantities. At the higher energy, however, one does observe the effect of orbital angular momentum in that the conservation law places a higher fraction of the total energy in translation than at 2.6 kcal; examination of our data indicates that the reactive cross section increases with energy and places more energy in translation, with ~55% of the total energy in translation. Contour maps in the c.m. system for IF production are shown in Figure 13.

The observation that the CH_3IF "molecule" must be stable with respect to the reactants $F + CH_3I$ is somewhat surprising initially. That the complex lives several rotational periods at a collision energy of 2.6 kcal $mole^{-1}$ tells us that it is bound by at least 20 kcal $mole^{-1}$. In a separate experiment (54), we have observed the production of CH_3IF in the endoergic bimolecular reaction $F_2 + CH_3I \rightarrow F + CH_3IF$. The energetics of this process and the corresponding reaction of atomic fluorine are shown in Figure 14. The energy scale which locates the stability of CH_3IF with respect to both reactions has been determined by integrating the differential cross section for CH_3IF production as a function of initial kinetic energy. Such measurements indicate that the threshold for CH_3IF formation is ~11 kcal, thus suggesting that the radical is stable with respect to $F + CH_3I$ by at least 25 kcal. Knowledge of the "well depth" of a "sticky" collision of this kind is generally unavailable and this technique of endoergic bimolecular synthesis appears to be of generality. In the final section of this paper, we discuss further development of this method for observing hitherto unknown free radical species.

B. A New Synthetic Method for Fluorine - Containing Radicals. The CH_3IF radical produced in the endoergic reaction of $F_2 + CH_3I$ is only one example of transient species produced in reactions of F_2 with other molecules. More recent work on similar systems involving trihalogens IIF and ClIF and the pseudo-trihalogen HIF has been performed (55,56), yielding information on the endoergic reactions

$$F_2 + I_2 \rightarrow IIF + F$$

$$F_2 + ICl \rightarrow ClIF + F$$

$$F_2 + HI \rightarrow HIF + F.$$

The IIF radical is of some importance in understanding the macroscopic reaction mechanism in the $F_2 + I_2$ system, particularly in view of predicted stabilities of trihalogen molecules from molecular orbital calculations (54), termolecular recombination work (58) and matrix isolation (59).

One must realize that the reaction

$$F_2 + XI \rightarrow XIF + F \quad (X = H, Cl, I)$$

can only yield observable XIF product if the decomposition of XIF into IF and X is endoergic. By measuring thresholds for the above reactions for X = H, Cl, I, we find values of 11, 6, and 4 kcal respectively and, further, the predominant products formed are XIF and F. The dissociation of XIF into IF + X at higher collision energies becomes important first for $F_2 + I_2$ at 7 kcal, and then for $F_2 + ICl$; the dissociation of HIF is an inaccessible channel for the collision energy range of these experiments.

In the $F_2 + ICl$ system, no product mass peaks at m/e 56 ($Cl^{37}F$) or m/e ($Cl^{35}F$) were observed and no m/e 20 (HF) peak was observed for the $F_2 + HI$ reaction. These mass spectral results indicate that the trihalogen and pseudo-trihalogen species formed involve bonding schemes such as ClIF and HIF with the more electropositive atom in the center of the molecule as predicted by Walsh's rules (60,61).

Figure 15 shows a contour map for the $F_2 + ICl$ system which is typical of all the data. Very forward peaked angular distributions for the products suggest that abstraction of an F atom from F_2 by XI proceeds through a somewhat bent geometry, i.e., F-F-I or F-I-X angle less than 180° in the system F-F-I-X.

Aside from the unique chemical identity of these trihalogens, the stability of the I_2F molecule is of importance in elucidating some features of the kinetics of the F_2/I_2 system (62). First of all, it is important to note that the gas phase generation of F atoms in F_2 and I_2 mixtures only requires 4 kcal of relative kinetic energy between F_2 and I_2 through the $F_2 + I_2 \rightarrow I_2F + F$ reaction. A recent study of this system indicates that electronically excited IF is formed as evidenced by chemiluminescence observations. The four center exchange reaction $F_2 + I_2 \rightarrow 2IF$ is exoergic by 60 kcal, more than enough to produce electronically excited IF, but our crossed molecular beam experiments have shown that at low energies collisions between $F_2 + I_2$ produce $I_2F + F$ or IF + I + F, but not 2IF. If I_2F were not stable, only the $F + I_2$ and $I + F_2$ reactions would be exoergic and then only by 30 kcal, too little to account for the chemiluminescence. However, the reaction $F + I_2F \rightarrow 2IF$ is exoergic by 64 kcal and, in view of the beam measurements of I_2F stability and the ease of production, could account for the observed chemiluminescence

in F_2 and I_2 mixtures.

Abstract

A summary of work in fluorine chemistry as determined from crossed molecular beam studies of reaction dynamics is presented. Special emphasis is given to studies of unimolecular decay of long-lived complexes formed from bimolecular association of fluorine atoms with unsaturated hydrocarbons. The experimental results are discussed in terms of statistical models for energy randomization in the complex as well as the role of the exit channel potential energy barrier in determining the product translational energy distribution.

Experimental results on recent studies of reactions of F_2 with a variety of species are also presented, with special attention to the utility of the method of endoergic bimolecular reactions in "synthesizing" unstable radicals such as trihalogens and pseudotrihalogens. Results are presented for $F_2 + I_2 \rightarrow I_2F + F$, $F_2 + HI \rightarrow HIF + F$, $F_2 + CH_3I \rightarrow CH_3IF$, and $F_2 + ICl \rightarrow FICl + F$.

Literature Cited

1. Lawley, K. P. ed, "Molecular Scattering", Adv. Chem. Phys. 30, Wiley, New York, 1975.
2. Molina, M. J., and Pimentel, G. C., IEEE J. Quantum Electron. (1973), QE9, 64.
3. Schafer, T. P., Siska, P. E., Parson, J. M., Tully, F. P., Wong, Y. C., and Lee, Y. T., J. Chem. Phys. (1970), 53, 3385.
4. Schafer, T. P., Ph.D. Dissertation, Univ. of Chicago (1972).
5. Polanyi, J. C., and Woodall, K. B., J. Chem. Phys. (1972), 57, 1574.
6. Jonathan, N., Melliar-Smith, C. M., and Slater, D. H., Mol. Phys. (1971), 20, 93.
7. Wilkins, R. L., J. Chem. Phys. (1972), 57, 912.
8. Muckerman, J. T., J. Chem. Phys. (1971), 54, 1155.
9. Schatz, G. C., Bowman, J. M., and Kuppermann, A., J. Chem. Phys. (1973), 58, 4023.
10. Bender, C. F., O'Neil, S. V., Pearson, P. K., and Schafer, H. F., J. Chem. Phys. (1972), 56, 4626.
11. Berry, M. J., J. Chem. Phys. (1973), 59, 6229.
12. Parson, J. M., and Lee, Y. T., J. Chem. Phys. (1972), 56, 4658.
13. Parson, J. M., Shobatake, K., Lee, Y. T., and Rice, S. A., J. Chem. Phys. (1973), 59, 1402.
14. Shobatake, K., Parson, J. M., Lee, Y. T., and Rice, S. A., J. Chem. Phys., (1973), 59, 1416.
15. Shobatake, K., Parson, J. M., Lee, Y. T., and Rice, S. A., J. Chem. Phys. (1973), 59, 1427.

16. Shobatake, K., Lee, Y. T., and Rice, S. A., J. Chem. Phys. (1973), 59, 1435.
17. Shobatake, K., Lee, Y. T., and Rice, S. A., J. Chem. Phys. (1973), 59, 6104.
18. Parson, J. M., Shobatake, K., Lee, Y. T., and Rice, S. A., Faraday Discuss. Chem. Soc. (1973), 55, 344.
19. Farrar, J. M., and Lee, Y. T., J. Chem. Phys. (1976), 65, 1414.
20. Morse, F. A., and Bernstein, R. B., J. Chem. Phys. (1962), 37, 2019.
21. Entemann, E. A., Ph.D. Dissertation, Harvard Univ. (1967).
22. Warnock, T. T., and Bernstein, R. B., J. Chem. Phys. (1968), 49, 1878.
23. Siska, P. E., Ph.D. Dissertation, Harvard Univ. (1969).
24. Farrar, J. M., and Lee, Y. T., Ann. Rev. Phys. Chem. (1974), 25, 357.
25. Lee, Y. T., McDonald, J. D., LeBreton, P. R., and Herschbach, D. R., Rev. Sci. Instrum. (1969), 40, 1402.
26. Anderson, J. B., Andres, R. P., and Fenn. J. B., Adv. Chem. Phys. (1969), 10, 289.
27. Mariella, R. P., Herschbach, D. R., and Klemperer, W., J. Chem. Phys. (1973), 58, 3785.
28. Bennewitz, H. G., Haerten, R., and Müller, G., Chem. Phys. Lett. (1971), 12, 335.
29. Schultz, A., Cruse, H. W., and Zare, R. N., J. Chem. Phys. (1972), 57, 1354.
30. Cruse, H. W., Dagdigian, P. J., and Zare, R. N., Faraday Discuss. Chem. Soc. (1973), 55, 277.
31. Hostettler, H. U., and Bernstein, R. B., Rev. Sci. Instrum. (1960), 31, 872.
32. Valentini, J. J., and Lee, Y. T., unpublished data.
33. Coombe, R. D., and Pimentel, G. C., J. Chem. Phys. (1973), 59, 251.
34. Coombe, R. D., and Pimentel, G. C., J. Chem. Phys. (1973), 59, 1535.
35. Fettis, G. C., Knox, J. H., and Trotman-Dickenson, A. F., J. Chem. Soc. London (1960), 1064.
36. Bender, C. F., O'Neil, S. V., Pearson, P. K., and Schaefer, H. F., Science (1972), 176, 1412.
37. Farrar, J. M., and Lee, Y. T., J. Chem. Phys. (1975), 63, 3639.
38. Forst, W., "Theory of Unimolecular Reactions", Academic New York, 1973.
39. Marcus, R. A., J. Chem. Phys. (1952), 20, 359.
40. Butler, J. N., and Kistiakowsky, G. B., J. Am. Chem. Soc. (1960), 82, 759.
41. Rynbrandt, J. D., and Rabinovitch, B. S., J. Chem. Phys. (1971), 54, 2275.
42. Pechukas, P., Light, J. C., and Rankin, C., J. Chem. Phys. (1966), 44, 794.

43. Lin, J., and Light, J. C., J. Chem. Phys. (1966), 45, 2545.
44. Wieder, G. M., and Marcus, R. A., J. Chem. Phys. (1966), 37, 1835.
45. Marcus, R. A., J. Chem. Phys. (1975), 62, 1372.
46. Shobatake, K., Rice, S. A., and Lee, Y. T., J. Chem. Phys. (1973), 59, 2483.
47. Jones, W. E., Macknight, S. D., Teng, L., Chem. Rev. (1973), 73, 407.
48. Williams, R. L., and Rowland, F. S., J. Chem. Phys. (1972), 76, 3509.
49. Light, J. C., private communication.
50. Bunker, D. L., J. Chem. Phys. (1972), 57, 332.
51. Leipunskii, I. O., Morozov, I. I., and Tal'rose, V. L., Dokl. Akad. Nauk. SSSR (1971), 198, 1367.
52. Miller, W. B., Safron, S. A., and Herschbach, D. R., Faraday Discuss. Chem. Soc. (1967), 44, 108.
53. McDonald, J. D., Ph.D. Dissertation, Harvard Univ. (1971).
54. Farrar, J. M., and Lee, Y. T., J. Am. Chem. Soc. (1974), 96, 7570.
55. Valentini, J. J., Coggiola, M. J., and Lee, Y. T., Faraday Discuss. Chem. Soc. (1976), to be published.
56. Valentini, J. J., Coggiola, M. J., and Lee, Y. T., J. Am. Chem. Soc. (1976), 98, 853.
57. Peyerimhoff, S. D., and Buenker, R. J., J. Chem. Phys. (1968), 49, 2473.
58. Bunker, D. L., and Davidson, N., J. Am. Chem. Soc. (1958), 80, 5090.
59. Nelson, L. Y., and Pimentel, G. C., J. Chem. Phys. (1967), 47, 3671.
60. Walsh, A. D., J. Chem. Soc. (1953), 2266.
61. Walsh, A. D., J. Chem. Soc. (1953), 2288.
62. Birks, J. W., Gabelnick, S. D., and Johnston, H. S., J. Mol. Spectr. (1975), 57, 23.

Figure Captions

1. Velocity vector Newton diagram showing relationship among the vectors $\underset{\sim}{u}$, $\underset{\sim}{v}$, and $\underset{\sim}{C}$.
2. Experimental arrangement for molecular beam studies of fluorine atom chemistry.
3. Upper panel: DF angular distributions at 0.80 kcal $mole^{-1}$ and 1.68 kcal $mole^{-1}$ collision energy. Lower panel: Cartesian flux contour maps generated from these data.
4. Schematic reaction coordinate for the system $F + C_2H_4$ relating the various energies of complex and critical configuration along the reaction coordinate.
5. Experimental angular distribution for C_2H_3F from $F + C_2H_4$ E_{rel} = 1.98 kcal $mole^{-1}$.
6. Center of mass contour map showing equal intensity points for formation of C_2H_3F from $F + C_2H_4$.

7. Experimental angular and TOF distribution data for F + C_2H_4 → C_2H_3F at 4 collision energies.
8. Schematic reaction coordinate diagram for the reactions of F + substituted benzenes.
9. Product recoil energy distributions for F + substituted benzenes.
10. IF product angular distribution from the reaction F + CH_3I at E_{rel} = 2.6 kcal $mole^{-1}$.
11. IF product angular distribution from the reaction F + CH_3I at E_{rel} = 14.1 kcal $mole^{-1}$.
12. IF product recoil energy distributions at E_{rel} = 2.6 and 14.1 kcal $mole^{-1}$. Best fit and model calculation distributions as noted.
13. C.M. contour map for IF production at 2.6 and 14.1 kcal $mole^{-1}$.
14. Schematic energy level diagram showing the relationship between the formation of CH_3IF as a transient species via the F + CH_3I path or as a stable radical via the F_2 + CH_3I pathway.
15. C.M. contour map for ClIF production from the reaction F_2 + ICl → ClIF + F at E_{rel} = 17.4 kcal $mole^{-1}$.

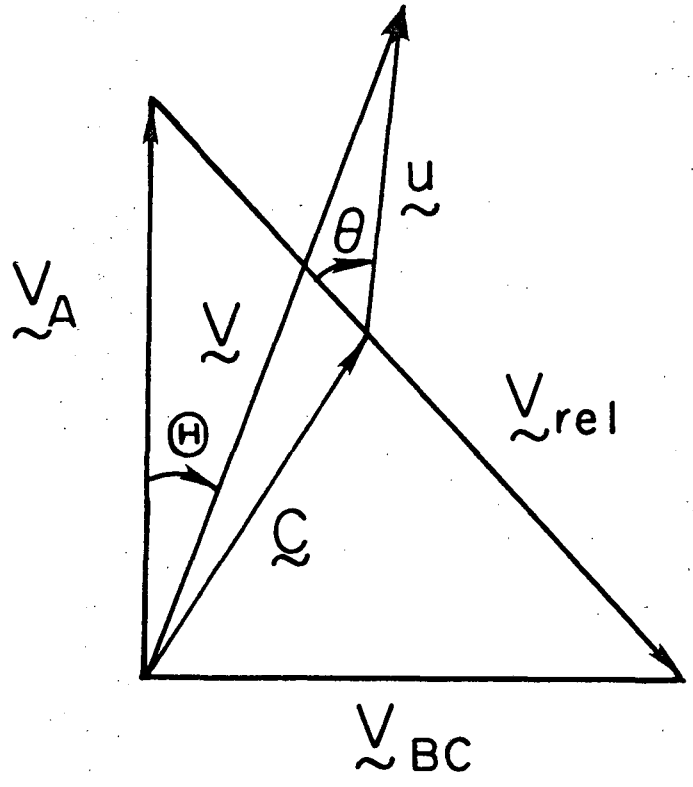

Fig. 1

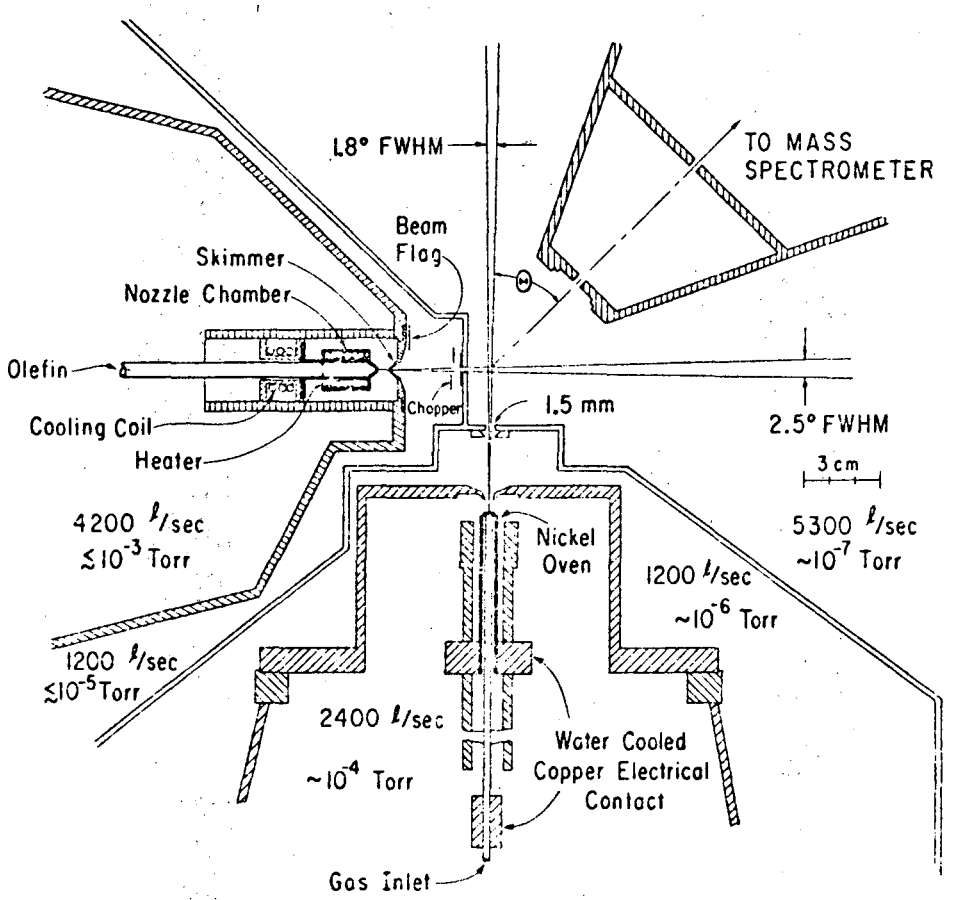

Fig. 2

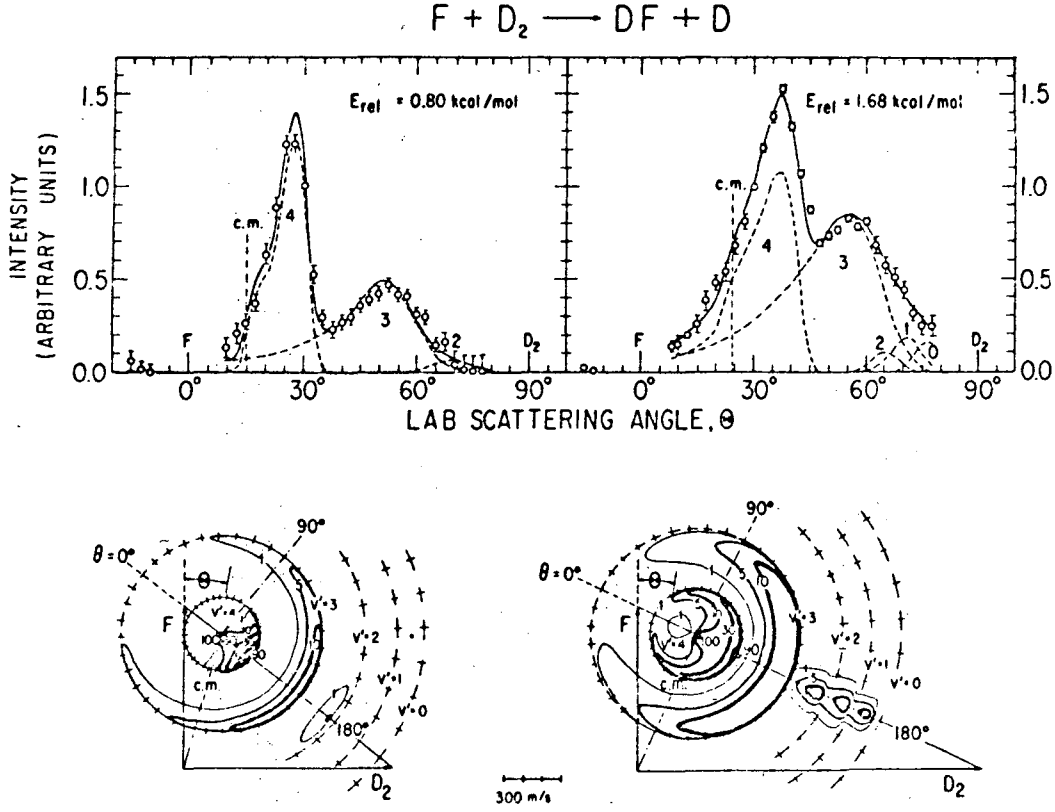
F + D2 ⟶ DF + D
INTENSITY (ARBITRARY UNITS)
Erel = 0.80 kcal/mol
Erel = 1.68 kcal/mol
c.m.
LAB SCATTERING ANGLE, Θ
θ=0°
90°
180°
F
D2
300 m/s

Fig. 3

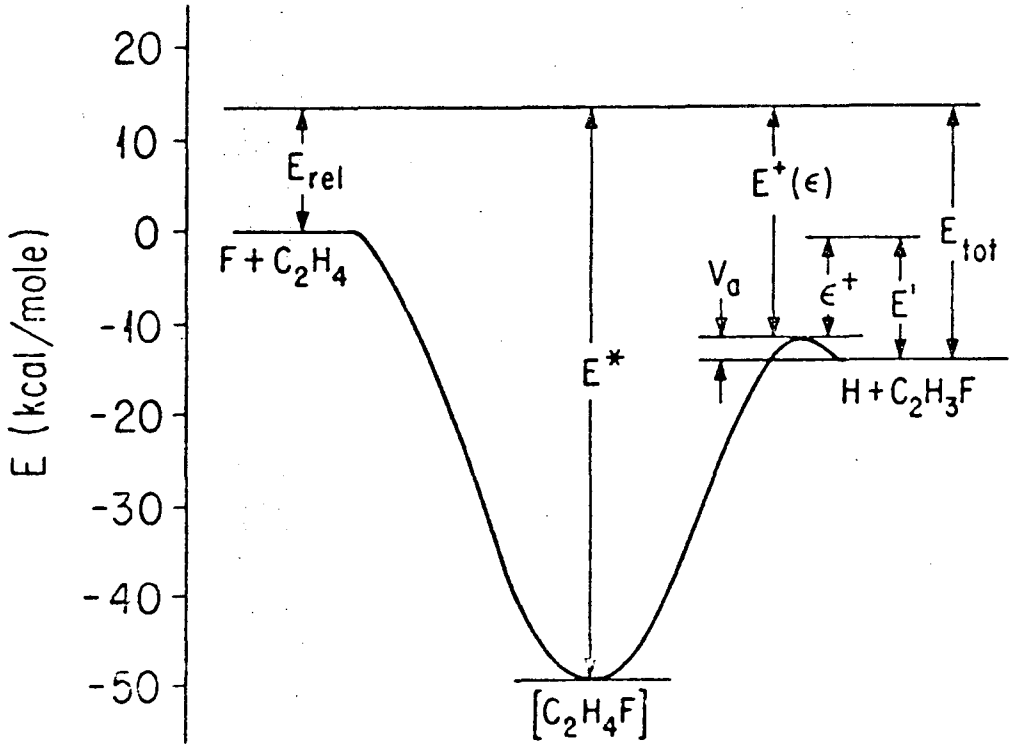
E (kcal/mole)
Erel
F + C2H4
E*
[C2H4F]
E+(ϵ)
Va
ϵ+
E'
Etot
H + C2H3F

Fig. 4

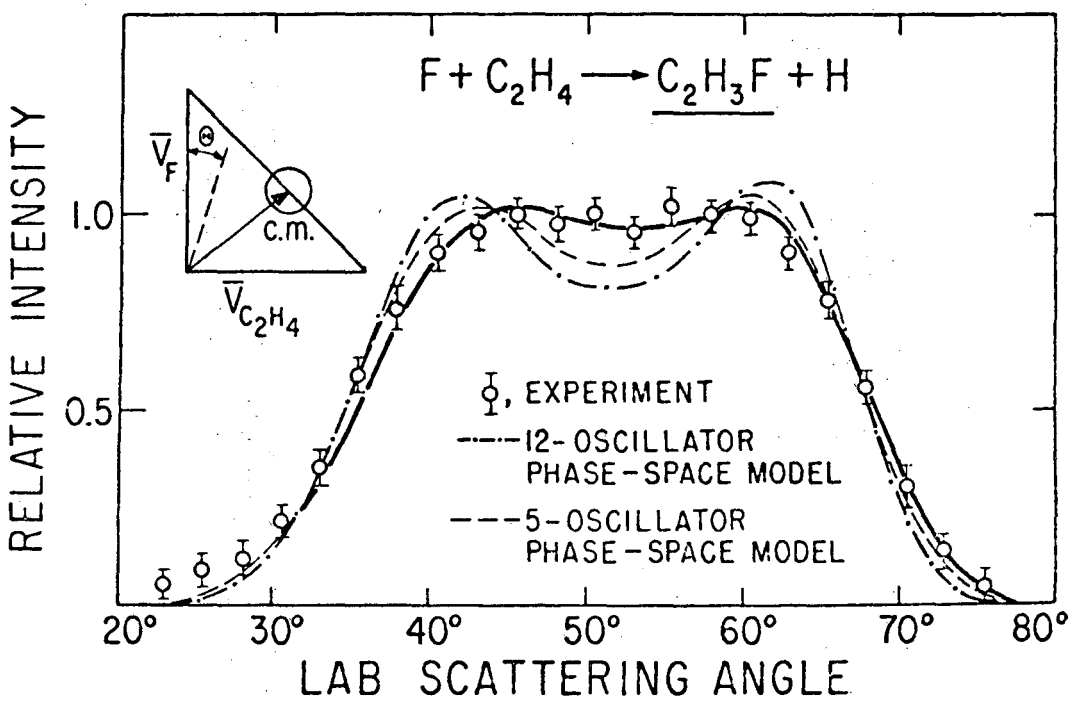

Fig. 5

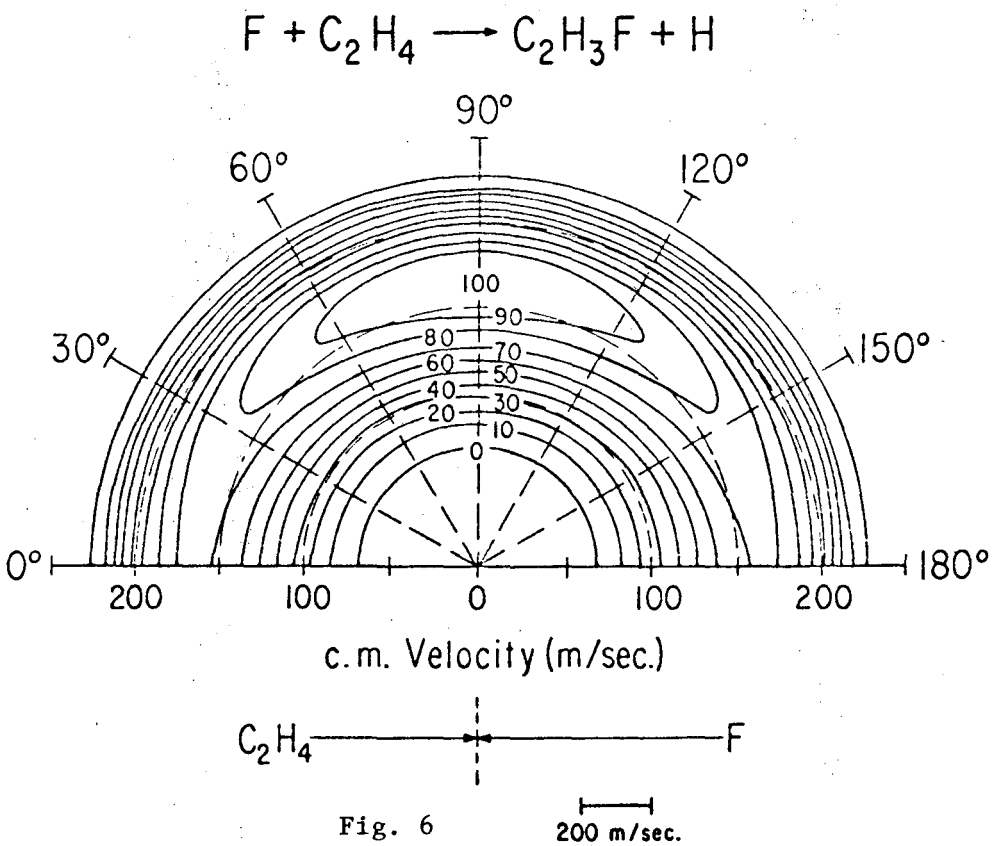

Fig. 6

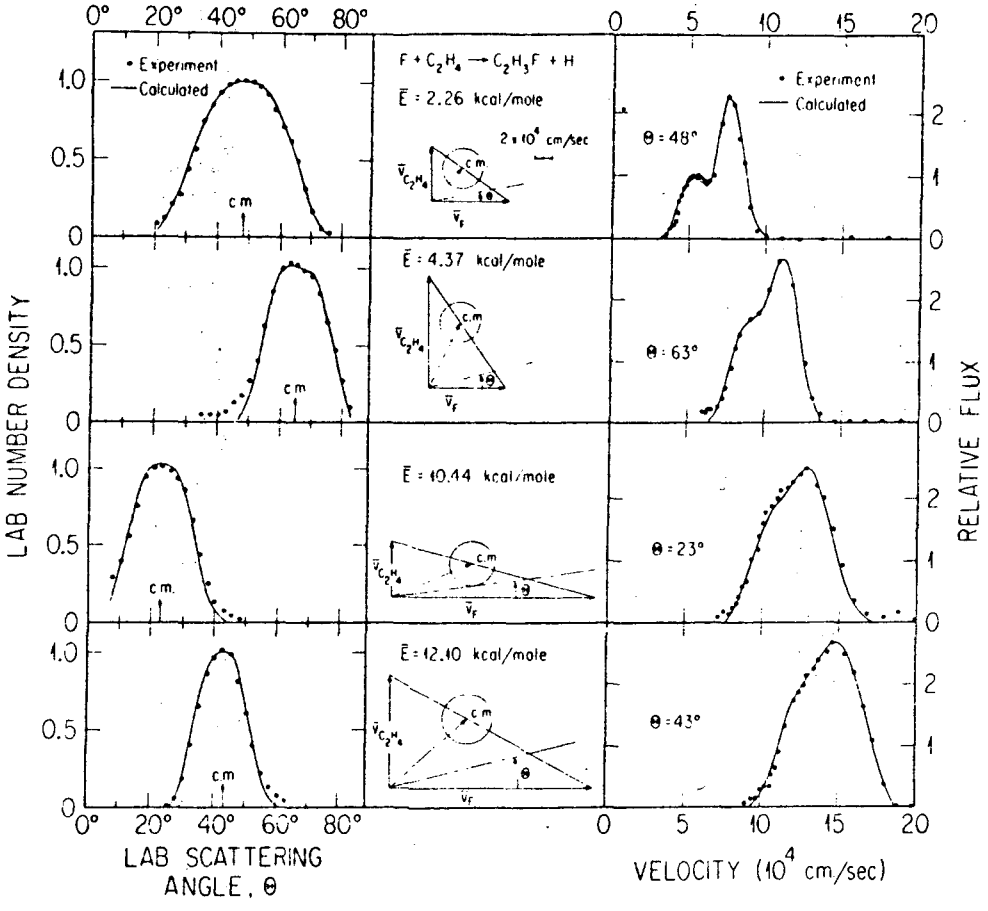
0° 20° 40° 60° 80°
0 5 10 15 20
• Experiment
— Calculated
F + C2H4 → C2H3F + H
Ē = 2.26 kcal/mole
2 × 10⁴ cm/sec
c.m
θ = 48°
Ē = 4.37 kcal/mole
θ = 63°
Ē = 10.44 kcal/mole
θ = 23°
Ē = 12.40 kcal/mole
θ = 43°
LAB NUMBER DENSITY
RELATIVE FLUX
LAB SCATTERING ANGLE, θ
VELOCITY (10⁴ cm/sec)

Fig. 7

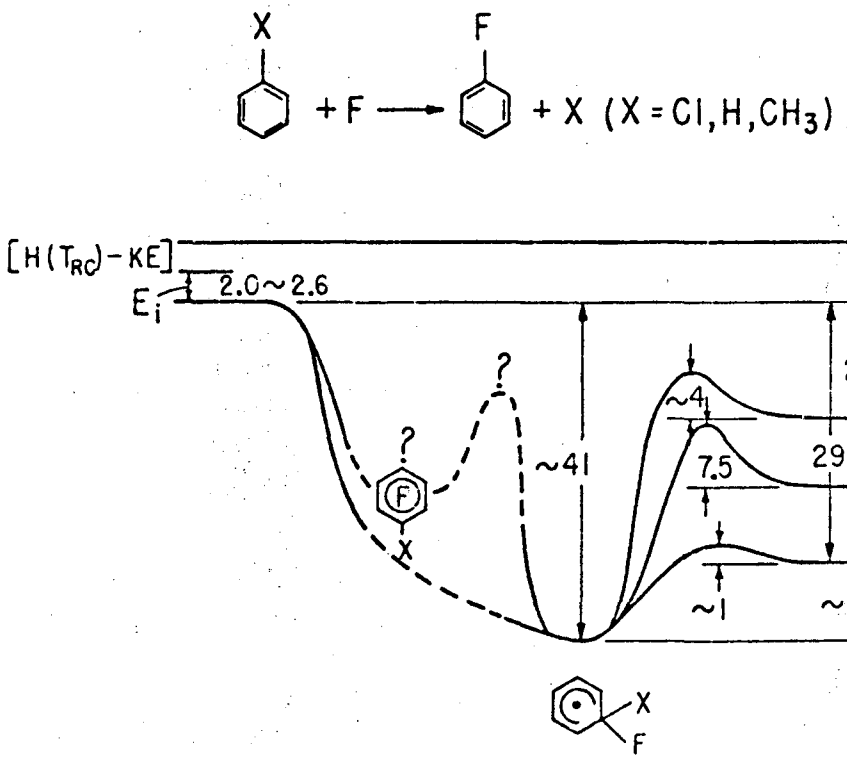

Fig. 8

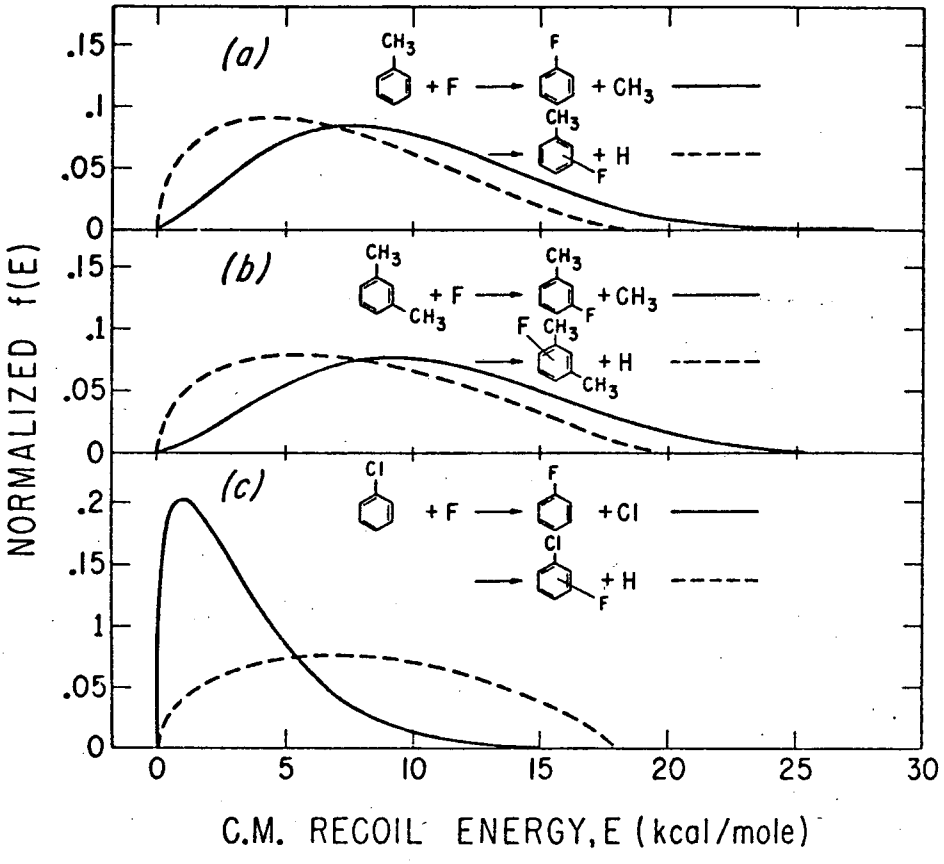
(a)
(b)
(c)
NORMALIZED f(E)
C.M. RECOIL ENERGY, E (kcal/mole)

Fig. 9

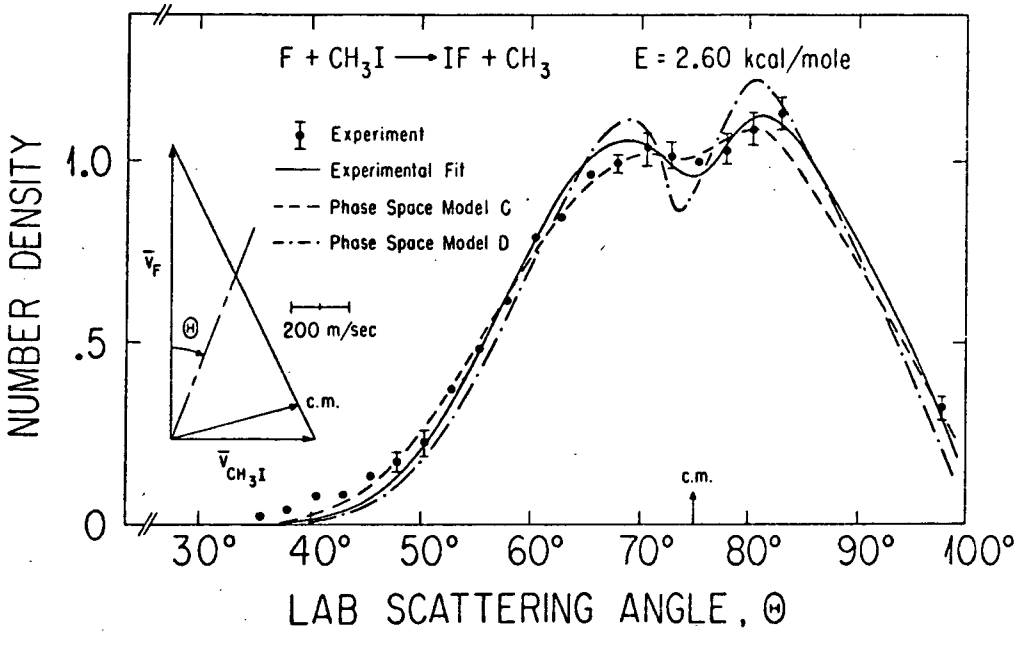
F + CH3I → IF + CH3
E = 2.60 kcal/mole
Experiment
Experimental Fit
Phase Space Model C
Phase Space Model D
200 m/sec
c.m.
NUMBER DENSITY
LAB SCATTERING ANGLE, Θ

Fig. 10

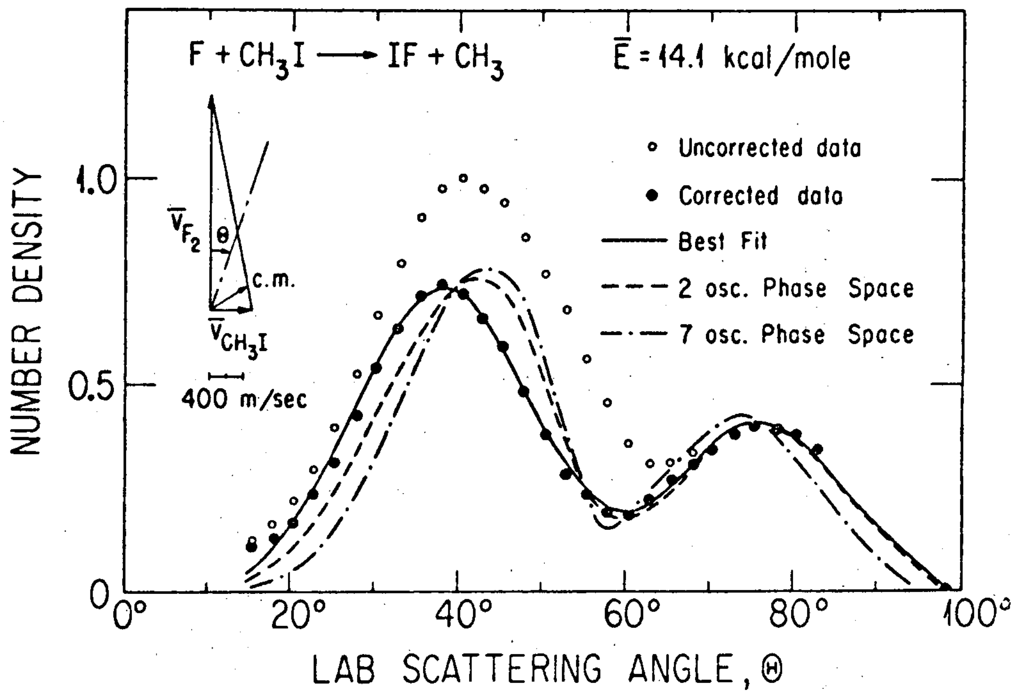

F + CH3I ⟶ IF + CH3
Ē = 14.1 kcal/mole
Uncorrected data
Corrected data
Best Fit
2 osc. Phase Space
7 osc. Phase Space
VF2
θ
c.m.
VCH3I
400 m/sec
NUMBER DENSITY
1.0
0.5
0
0°
20°
40°
60°
80°
100°
LAB SCATTERING ANGLE, Θ

Fig. 11

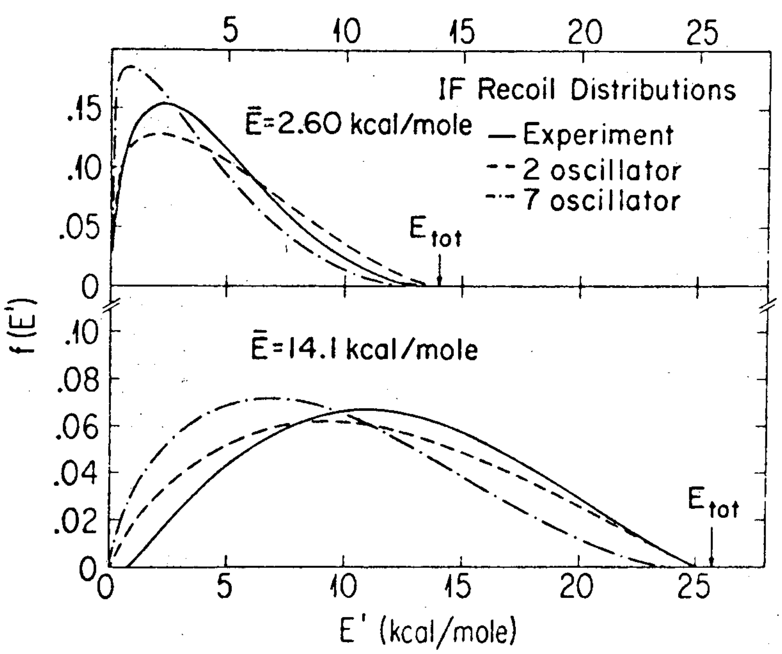

IF Recoil Distributions
Ē=2.60 kcal/mole
Experiment
2 oscillator
7 oscillator
Etot
Ē=14.1 kcal/mole
f(E')
E' (kcal/mole)

Fig. 12

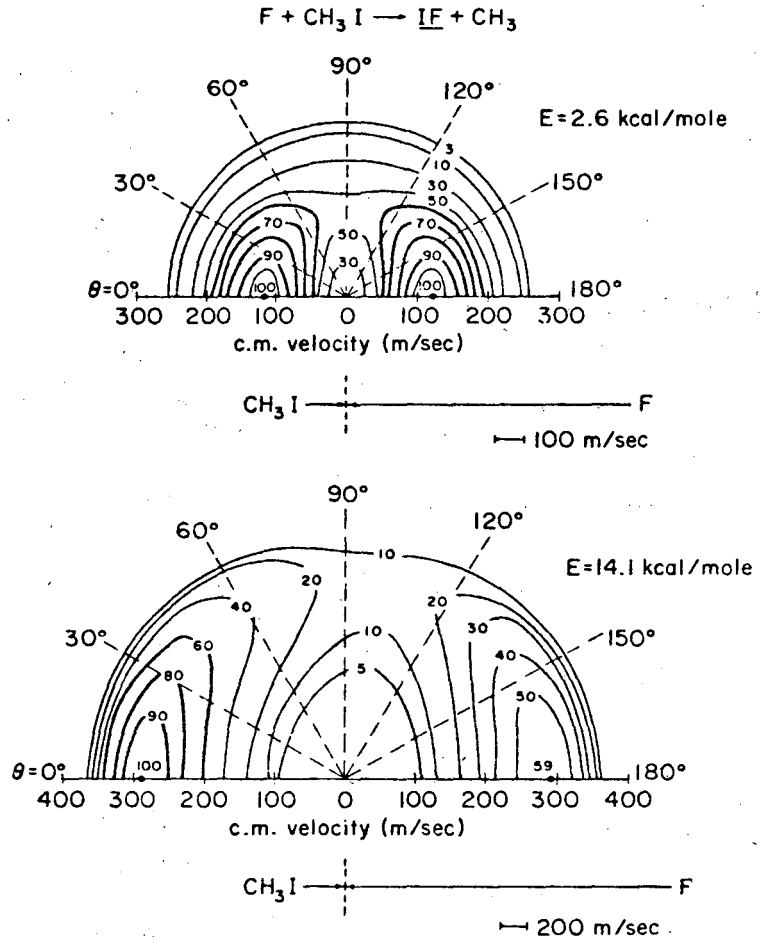
F + CH3 I → IF + CH3
90°
60°
120°
E=2.6 kcal/mole
30°
150°
3
10
30
50
70
90
100
θ=0°
180°
300 200 100 0 100 200 300
c.m. velocity (m/sec)
CH3 I
F
100 m/sec
90°
60°
120°
E=14.1 kcal/mole
10
20
40
30°
150°
60
80
90
100
5
30
50
59
θ=0°
180°
400 300 200 100 0 100 200 300 400
c.m. velocity (m/sec)
CH3 I
F
200 m/sec

Fig. 13

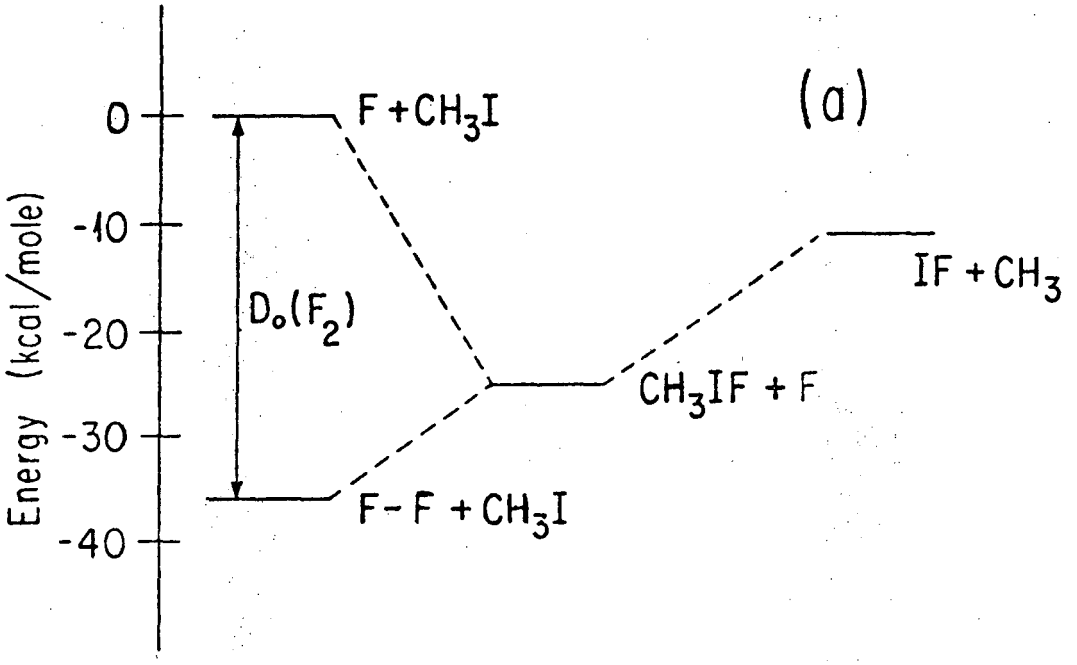
0
-10
-20
-30
-40
Energy (kcal/mole)
F + CH3I
(a)
D0(F2)
IF + CH3
CH3IF + F
F - F + CH3I

Fig. 14

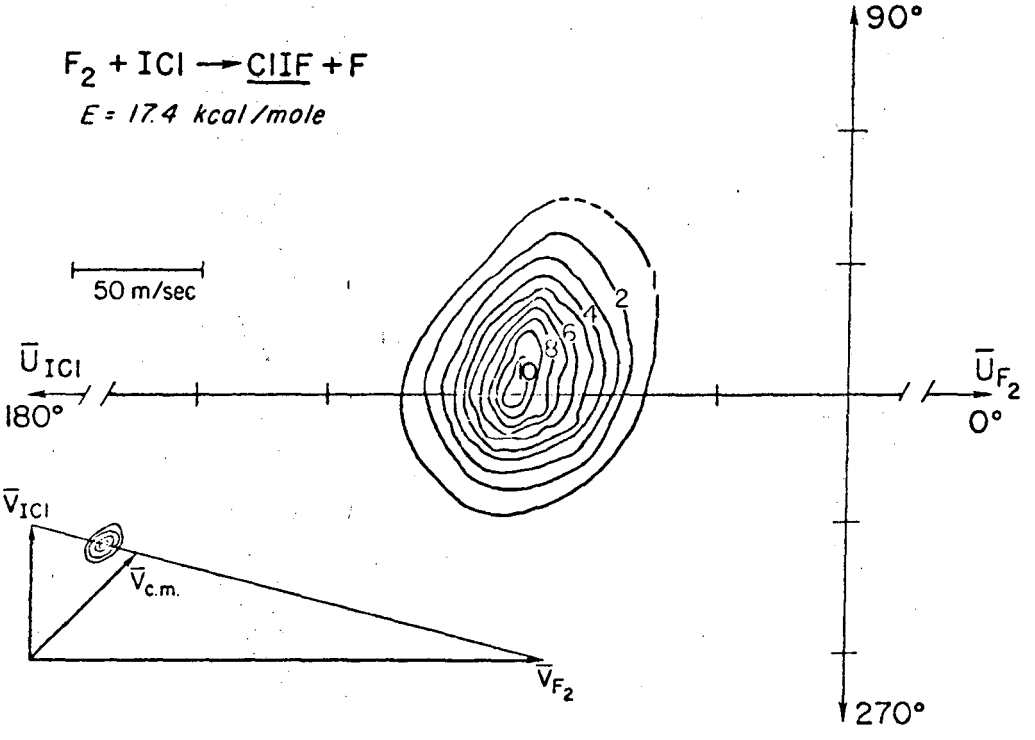
F2 + ICl → ClIF + F
E = 17.4 kcal/mole
50 m/sec
90°
180°
0°
270°
2
4
6
8
10
V̄ICl
V̄c.m.
V̄F2
XBL 764-2678

Fig. 15

TECHNICAL INFORMATION DIVISION
LAWRENCE BERKELEY LABORATORY
UNIVERSITY OF CALIFORNIA
BERKELEY, CALIFORNIA 94720